SEMARAK ILMU PUBLISHING

Semarak Journal of Thermal-Fluid Engineering

Journal homepage:
https://semarakilmu.my/index.php/sjotfe/index
ISSN: 3030-6639

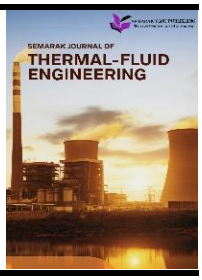

Analysis of Conjugate Heat Transfer in a Simplified Heat Exchanger

Ahmad Alif Ashraf Azwan[1], Ishkrizat Taib[1,2*], Ahmad Danial Ahmad Junaidi[1], Ahmad Nadzim Jaafar[1], Aiman Akmal Mohd Farez[1], Eng Shao Tang[1]

[1] Faculty of Mechanical and Manufacturing Engineering, Universiti Tun Hussein Onn Malaysia, 86400 Parit Raja, Batu Pahat, Johor, Malaysia
[2] UTHM-INTEKMA Advanced Industrial Modelling, Faculty of Mechanical and Manufacturing Engineering, Universiti Tun Hussein Onn Malaysia, 86400 Parit Raja, Batu Pahat, Johor, Malaysia

ARTICLE INFO

Article history:
Received 16 January 2026
Received in revised form 20 February 2026
Accepted 15 March 2026
Available online 31 March 2026

Keywords:
Conjugate heat transfer (CHT); heat exchanger; CFD; heat transfer rate; thermal performance

ABSTRACT

This study presents a Computational Fluid Dynamics (CFD) investigation of conjugate heat transfer (CHT) in a simplified serpentine heat exchanger under varying geometric configurations and thermal operating conditions. The objective of this research is to examine how the number of passes affects the exchanger's thermal performance, temperature distribution, and total heat transfer rate. Three configurations of 3-pass, 5-pass, and 7-pass simplified heat exchangers were designed using copper as the solid wall material and water as the tube-side working fluid. Simulations were conducted under three thermal sets with inlet and shell temperatures of 25 °C/70 °C, 15 °C/90 °C, and 10 °C/120 °C, respectively. The inlet velocity was fixed at 1 m/s, corresponding to a constant mass flow rate of 10.113 kg/s, to ensure consistent flow conditions across all cases. The results revealed that increasing the number of passes substantially enhanced heat transfer performance due to extended flow residence time and increased surface area for heat exchange. In the high-temperature difference case (10 °C/120 °C), the outlet temperature increases from 17.66 °C for the 3-pass design to 20.20 °C for the 7-pass design. Consequently, the total heat transfer rate increased from 323.96 kW to 431.38 kW, indicating a 33 % enhancement in energy absorption. Similarly, under moderate and low temperature differences, the heat transfer rates increased by 32 % and 54 %, respectively, when the pass number increased from 3 to 7. These findings confirm that the 7-pass configuration provides the most effective heat absorption across all thermal conditions. Overall, the study demonstrates that optimizing pass arrangement and flow path length significantly improves conjugate heat transfer efficiency in the simplified heat exchangers.

1. Introduction

Conjugate heat transfer (CHT) is a fundamental area of thermal–fluid science that deals with the simultaneous interaction between convective heat transfer in fluid domains and conductive heat transfer within solid structures. It plays a crucial role in analyzing and designing engineering systems such as heat exchangers, cooling channels, electronic thermal management devices, and energy conversion equipment, where the thermal response of the solid is strongly coupled with the

* *Corresponding author.*
E-mail address: iszat@uthm.edu.my

https://doi.org/10.37934/sjotfe.8.1.3142a

surrounding fluid flow [1]-[5]. Accurate prediction of temperature distribution, heat flux, and thermal gradients at fluid–solid interfaces is essential for evaluating system performance, thermal efficiency, and structural reliability under operating conditions.

The thermal behaviour in CHT problems is governed by the coupled solution of momentum and energy transport in fluids and heat conduction in solids. Key influencing parameters include flow regime, fluid properties, thermal conductivity of the solid, boundary conditions, and geometric configuration. In practical heat exchanger applications, flow may be laminar or turbulent, leading to non-uniform temperature fields and localised heat transfer enhancement or degradation along the solid walls [6]-[9]. Simplified analytical solutions and empirical correlations often assume idealised boundary conditions such as constant wall temperature or uniform heat flux, which are insufficient to capture the complex thermal interactions occurring in real conjugate systems, particularly in geometries involving internal flow passages and thick solid walls.

Computational Fluid Dynamics (CFD) has emerged as a powerful and widely adopted tool for analysing conjugate heat transfer problems, as it enables the simultaneous numerical solution of the continuity, momentum, and energy equations across both fluid and solid domains. Using discretisation techniques such as the finite volume method, CFD can resolve detailed velocity fields, temperature distributions, and heat flux continuity at the fluid–solid interface, providing a more realistic representation of thermal behaviour compared to decoupled or one-way heat transfer approaches [10],[11]. The accuracy of CFD-based CHT simulations depends strongly on mesh quality, numerical schemes, turbulence modelling, and appropriate treatment of interfacial coupling between the fluid and solid regions. Previous studies have emphasised that mesh refinement near the fluid–solid interface and in regions of high thermal gradients is critical for accurately capturing wall temperature variation and local heat transfer rates [12]-[14].

Therefore, this study aims to investigate conjugate heat transfer behaviour in a simplified heat exchanger using Computational Fluid Dynamics (CFD). Three different heat exchanger designs are analysed under three distinct sets of thermal operating parameters. The inlet fluid velocity is maintained constant to ensure comparable flow conditions across all cases. The simulations focus on analysing temperature distribution contours and total heat transfer through the solid walls. The results provide insight into fluid–solid thermal interactions and demonstrate the capability of CFD to predict conjugate heat transfer performance in practical heat exchanger applications.

2. Methodology

2.1 Geometry of Computational Domain for the Simplified Heat Exchanger

The computational domain for this study was created to represent a simplified heat exchanger with serpentine flow passages, as shown in Figure 1. Three different geometric configurations were considered, consisting of 3-pass, 5-pass, and 7-pass pipe arrangements. These configurations were selected to examine the effect of the number of passes on heat transfer performance while maintaining the same basic layout. Each model consists of an internal fluid domain representing water flow and a surrounding solid domain representing the copper walls of the heat exchanger. The serpentine design increases the total flow length, allowing the fluid to interact repeatedly with the heated solid surface. As the number of passes increases from 3 to 7, the overall flow path length and contact area between the fluid and the solid wall increase correspondingly. This setup ensures a consistent comparison between the three designs, so that differences in temperature distribution and heat transfer are primarily influenced by the number of passes.

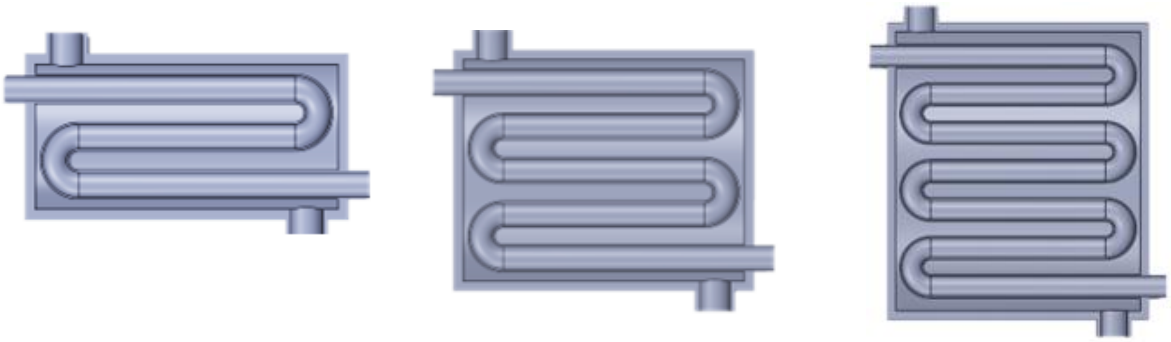

(a) (b) (c)

Fig. 1. Computational domain of the simplified heat exchanger (a) 3-Pass (b) 5-Pass (c) 7-Pass

2.2 Discretization

In this study, the heat exchanger domain was discretized to enable numerical solution of the coupled fluid and solid energy equations. Three simplified serpentine heat exchanger configurations were considered, namely the 3-Pass, 5-Pass, and 7-Pass designs. The internal fluid passages and surrounding solid walls were divided into finite control volumes using an automated polyhedral mesh, generated through the ANSYS Watertight Geometry workflow. This approach ensures robust handling of complex geometries while maintaining clear separation between fluid and solid regions, which is essential for reliable conjugate heat transfer analysis.

2.2.1 Mesh generation of the simplified heat exchanger

The watertight meshing process produced a hybrid mesh comprising structured elements in geometrically simple regions and unstructured elements in areas of higher complexity, such as serpentine bends. Mesh refinement was applied at fluid-solid interfaces to accurately capture heat flux and temperature gradients between the liquid water (H_2O) and the copper walls. Inflation layers were included along the channel walls to resolve near-wall thermal boundary layers effectively. As the number of passes increased from 3 to 7, mesh density was adjusted accordingly to maintain solution accuracy and numerical stability. Mesh adequacy was verified through smooth temperature contours and stable convergence behaviour, confirming that the applied meshing strategy provided sufficient resolution for all configurations. Figure 2 show the meshing of heat exchanger.

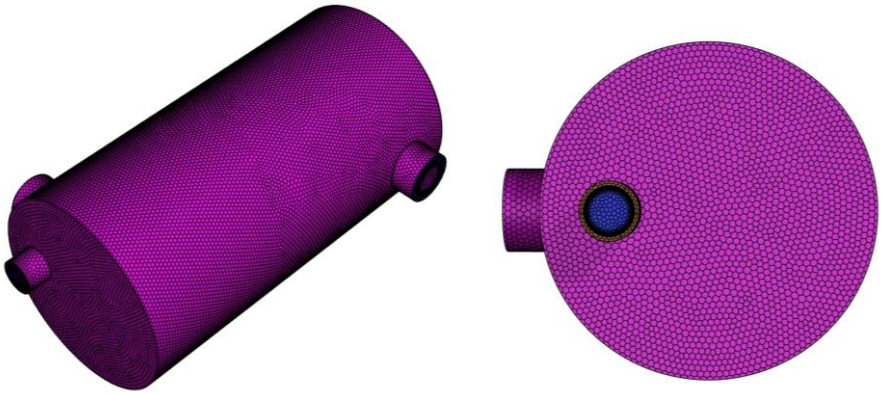

(a) (b)

Fig. 2. Computational mesh of the simplified heat exchanger (a) Isometric (b) Front view

2.2.2 Grid independence test

The Grid Independence Test (GIT) is an important step in Computational Fluid Dynamics (CFD) analysis to ensure that the numerical results are not influenced by the mesh size or grid resolution. In this process, simulations are performed using different mesh densities while keeping the boundary conditions and physical parameters constant. When further refinement of the mesh results in negligible changes in the key parameters, the solution is considered grid independent. Conducting a GIT helps balance accuracy and computational efficiency by selecting a mesh that provides reliable results without unnecessary computational cost [15]-[17].

2.3 Governing Equation

In this study, a conjugate heat transfer (CHT) formulation is employed to analyse heat transfer in a simplified heat exchanger, which involves internal fluid flow, external fluid flow, and heat conduction through a solid wall. The governing equations consist of the conservation equations for mass, momentum, and energy in the fluid domains, together with the heat conduction equation in the solid domain. These equations are derived from first principles and are commonly applied to internal and external flow problems in CFD analysis [18].

2.3.1 Continuity equation

The continuity equation represents the conservation of mass. For an incompressible fluid with constant density, the continuity equation is expressed as:

$$\nabla . u = 0 \tag{1}$$

where u is the velocity vector. This equation ensures that mass is conserved throughout the fluid domain and applies to both internal flow inside the heat exchanger passage and external flow over the solid surfaces.

2.3.2 Momentum equation (Navier-Stokes)

The conservation of momentum in the fluid domains is governed by the incompressible Navier–Stokes equations:

$$\rho \left(\frac{\partial \vec{V}}{\partial t} + u . \nabla u \right) = -\nabla \mathrm{p} - \mu \nabla^2 u \tag{2}$$

where ρ is the fluid density, p is the static pressure, and μ is the dynamic viscosity. This equation is widely used to model internal and external flows in engineering applications, including flow inside heat exchanger channels and flow around solid walls.

2.3.3 Energy equation (fluid domain)

The temperature distribution in the fluid is governed by the energy conservation equation, which accounts for heat transfer by convection and conduction:

$$\rho c_p \left(\frac{\partial T}{\partial t} + u \cdot \nabla T\right) = k_f \nabla^2 T \quad (3)$$

For where c_p is the specific heat capacity, T is the temperature, and k_f is the thermal conductivity of the fluid. This equation is solved in both internal and external flow regions to capture heat transfer between the fluid and the heat exchanger wall.

2.3.4 Heat conduction equation (solid domain)

Heat transfer within the solid wall of the heat exchanger is modelled using the heat conduction equation, which describes energy transport within stationary solids:

$$\rho_s c_{p,s} \frac{\partial T_s}{\partial t} = k_s \nabla^2 T_s \quad (4)$$

where ρ_s, $c_{p,s}$, and k_s represent the density, specific heat capacity, and thermal conductivity of the solid material, respectively, and T_s is the solid temperature. In the solid domain, heat transfer occurs solely by conduction, and no fluid motion is present [19]:

2.3.5 Fluid-solid interface coupling conditions

At the interface between the fluid and solid domains, conjugate heat transfer is achieved by enforcing continuity conditions for both temperature and heat flux, ensuring physically consistent thermal interaction between internal flow, external flow, and the solid wall [5].

Temperature continuity:

$$T_f = T_s \quad (5)$$

Heat flux continuity:

$$k_f \frac{\partial T_f}{\partial n} = k_s \frac{\partial T_s}{\partial n} \quad (6)$$

where the subscripts f and s denote the fluid and solid domains, respectively, and n is the direction normal to the interface. These interface conditions are a defining feature of conjugate heat transfer analysis and are commonly applied in CFD simulations of heat exchangers [20].

2.4 Boundary Condition

Consistent boundary conditions were applied to all three heat exchanger configurations to ensure a fair comparison of thermal performance [21]. Liquid water was selected as the working fluid, while copper was assigned as the solid material for the heat exchanger walls. A uniform inlet velocity of 1 m/s was imposed at the fluid inlet, establishing a forced convection regime throughout the exchanger. Three sets of thermal operating parameters were considered to evaluate performance under different temperature differences: the first set had a cold-fluid inlet temperature of 15 °C and a hot-fluid inlet temperature of 90 °C, the second set had 25 °C and 70 °C, and the third set had 10 °C and 120 °C. Pressure outlet boundary conditions with a gauge pressure of 0 Pa were applied at the outlets, allowing the flow to develop naturally within the exchanger. All fluid–solid interfaces were

treated as perfectly bonded, ensuring continuous heat flux and temperature coupling between the copper walls and the water flow.

2.5 Analysis
2.5.1 Temperature analysis

Temperature distribution is a key parameter in understanding conjugate heat transfer behaviour in the heat exchanger. Temperature contours reflect how thermal energy is transferred between the fluid and solid walls and indicate regions of high and low heat transfer [22]. Extracting temperature contours along the fluid and solid domains allows identification of thermal gradients, hotspots, and regions of uniform heat distribution. Analysing these contours provides insight into the effectiveness of heat transfer for different heat exchanger designs and highlights the influence of the number of passes on the overall thermal performance [23].

2.5.2 Heat transfer rate (Q) analysis

The total heat transfer rate, Q, is an important quantitative measure of the thermal performance of the heat exchanger [24]. By evaluating Q for each configuration, the study quantifies the amount of energy transferred from the hot fluid to the cold fluid through the solid wall. Comparing Q values between the 3-pass, 5-pass, and 7-pass designs allows assessment of the impact of flow path length, surface area, and residence time on heat exchange efficiency. This analysis provides a direct metric for design performance and can guide optimization of heat exchanger geometry.

2.5.3 Heat transfer performance analysis

The thermal performance of the heat exchanger is strongly influenced by both the geometric configuration and the flow path of the tube-side fluid [25]. The number of passes directly affects the residence time, defined as the average duration a fluid particle remains within the heat transfer domain. Longer residence times, achieved with higher-pass designs, allow the fluid to stay in contact with the hot shell-side fluid for an extended period, promoting more thorough heat transfer from the walls to the bulk fluid. In addition, the available heat transfer surface area increases with the number of passes, as the fluid travels a longer distance within the tubes. This larger surface area provides more interface for energy exchange [26]-[28], enhancing the overall heat transfer efficiency. By analysing both the residence time and surface area effects, it is possible to explain the observed differences in outlet fluid temperatures and total energy absorbed between the 3-pass, 5-pass, and 7-pass configurations, demonstrating how geometric modifications can effectively improve heat exchanger performance.

3. Results
3.1 Grid Independence Test Result

The grid independence test was performed to ensure that the numerical results obtained from the conjugate heat transfer simulations are not significantly affected by mesh resolution [29]. In this study, the pressure drop of the tube-side fluid was selected as the monitoring parameter, as it is highly sensitive to mesh refinement in internal flows, particularly in serpentine geometries involving multiple bends and extended wall interaction. Tables 1 to 3 shows the pressure drop obtained using three different mesh densities under identical boundary conditions. The results show that the coarser

mesh predicts a slightly different pressure drop due to limited resolution near the tube walls and curved sections. With further mesh refinement, the predicted pressure drop converges, and the results from the medium and fine meshes show very close agreement. This indicates that additional mesh refinement does not produce significant changes in the pressure drop prediction.

Table 1
Grid independence test for the 3-pass heat exchanger

Node	P_{in}, Pa	P_{out}, Pa	ΔP, Pa	Truncation error
748441	1419.0172	750.55109	668.46611	
2556344	1843.041	747.91344	1095.12756	0.3896
17486585	2275.1289	725.00935	1550.11955	0.2935

Table 2
Grid independence test for the 5-pass heat exchanger

Node	P_{in}, Pa	P_{out}, Pa	ΔP, Pa	Truncation error
1448864	1400.2748	754.01963	646.25517	
5789386	1836.502	727.31333	1109.18867	0.4174
41279089	2192.3143	717.10244	1475.21186	0.2481

Table 3
Grid independence test for the 7-pass heat exchanger

Node	P_{in}, Pa	P_{out}, Pa	ΔP, Pa	Truncation error
2383099	1335.7523	722.44083	613.31147	
10870772	1866.8282	730.28876	1136.53944	0.4604
79166081	2232.3143	710.113	1522.2013	0.2534

Based on the grid independence assessment, the medium mesh was selected for all subsequent simulations to reduce computational cost while maintaining numerical accuracy. The difference in predicted pressure drops between the medium and fine meshes was found to be very small, with a deviation below 0.3 for all designs, which indicates that further mesh refinement produces negligible improvement in the solution. This confirms that the medium mesh provides a suitable balance between solution accuracy and computational efficiency for the present conjugate heat transfer analysis.

3.2 Temperature Contour of Three Different Designs and Parameters

The temperature contours illustrate the effect of both heat exchanger design and operating temperature on the thermal behaviour of the tube-side fluid. Figures 3 to 5 show the temperature distribution for the 3-Pass, 5-Pass, and 7-Pass heat exchanger configurations under three different inlet–shell temperature sets, which are 15-90 °C, 25-70 °C, and 10-120 °C. These cases are used to examine the influence of flow path length and temperature difference on the development of the thermal boundary layer, heat penetration into the fluid core, and overall energy absorption. By comparing the temperature fields across all designs and operating conditions, the effectiveness of each configuration in promoting thermal energy transfer from the shell to the tube-side fluid can be clearly observed.

For the first temperature set (15-90°C), the 3-Pass design in Figure 5 exhibits a dominant cold core throughout the tube, with only a thin light-blue boundary layer along the walls. This indicates that the short flow path and limited residence time restrict heat penetration into the bulk fluid. The 5-Pass design in Figure 4 shows thicker boundary layers and partial warming of the core, although most of the fluid remains cooler than the walls. In contrast, the 7-Pass design in Figure 3

demonstrates significantly improved thermal development, with the wall-adjacent fluid progressing through cyan and green regions and the core showing noticeable warming, indicating effective heat transfer from the shell.

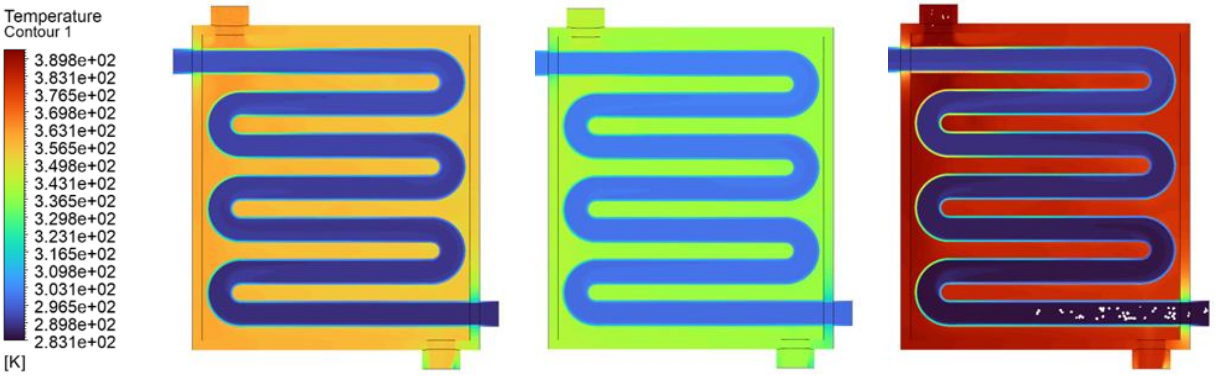

(a) (b) (c)

Fig. 3. Temperature contour (a) Medium (b) Low (c) High temperature differences for 7-pass design

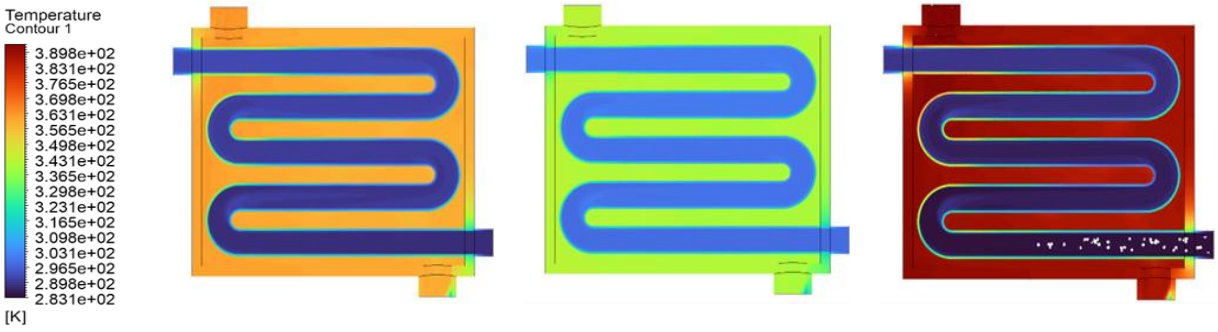

(a) (b) (c)

Fig. 4. Temperature contour (a) Medium (b) Low (c) High temperature differences for 5-pass design

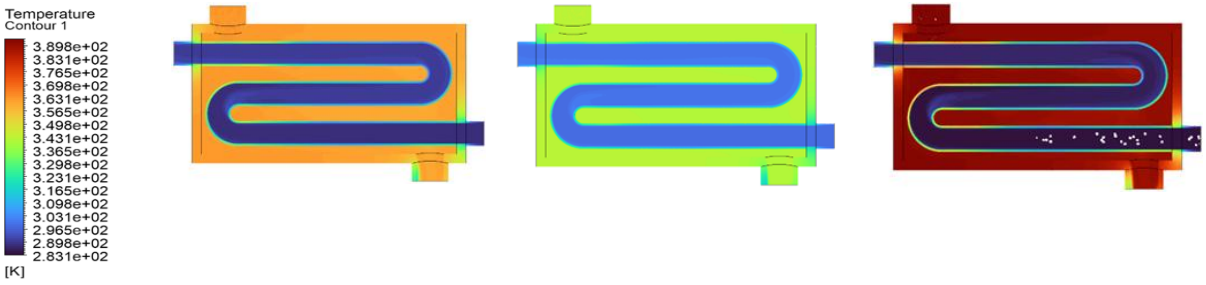

(a) (b) (c)

Fig. 5. Temperature contour of (a) Medium (b) Low (c) High temperature differences for 3-pass design

In the second temperature set (25-70 °C), the driving force is lower, resulting in generally softer temperature gradients across all designs. The 3-Pass design still shows minimal core warming, with the thermal boundary layer remaining thin and light blue. The 5-Pass design achieves slightly better heating, with more pronounced cyan regions along the walls, but the fluid core remains largely underdeveloped. The 7-Pass design again demonstrates the most uniform thermal penetration, with the boundary layers expanding and the core fluid shifting towards green hues, indicating that even with a reduced temperature difference, the extended flow path facilitates improved energy absorption.

Lastly, for the third temperature set (10-120 °C), the high thermal driving force produces strong temperature gradients. The 3-Pass design shows limited improvement compared to the other sets,

with the core remaining predominantly blue, but the wall regions reach warmer colours due to the large ΔT. The 5-Pass design captures more heat, with wider cyan and light-green regions along the walls, and the core begins to warm slightly. The 7-Pass configuration exhibits the most substantial thermal penetration, with wall-adjacent fluid approaching yellow-red hues and the core showing distinct warming, indicating that the combination of a long flow path and high driving force maximizes heat transfer efficiency.

Overall, comparison across all three temperature sets confirms that the number of passes plays a dominant role in thermal development, while the inlet-to-shell temperature difference primarily affects the magnitude of heat absorbed. The 7-Pass design consistently provides the most effective thermal penetration, followed by the 5-Pass design, whereas the 3-Pass design remains thermally underdeveloped in all cases. These observations highlight the combined influence of geometric configuration and operating conditions on the heat transfer performance of simplified serpentine heat exchangers**.**

3.3 Heat Transfer Rate (Q) Analysis

The total heat transfer rate, Q, represents the amount of thermal energy transferred from the hot shell-side fluid to the cold tube-side fluid and serves as a key indicator of the heat exchanger's performance [30],[31]. By evaluating the heat transfer rate for the different heat exchanger designs and operating conditions, it is possible to quantify the influence of geometric parameters, such as the number of passes, on thermal efficiency. This analysis allows a direct comparison of energy absorption across the 3-Pass, 5-Pass, and 7-Pass configurations, highlighting how residence time, surface area, and flow interactions contribute to overall heat transfer. Tables 4 to 6 provide the result of the heat transfer rate that has been extracted from the simulation.

Table 4
Low temperature difference case (25 °C inlet / 70 °C shell)

Design	Outlet temperature, °C	Mass flow rate, kg/s	Heat transfer rate, kW
3-Pass	27.21	10.113	93.47
5-Pass	27.92	10.113	123.49
7-Pass	28.41	10.113	144.22

Table 5
Medium temperature difference case (15 °C inlet / 90 °C shell)

Design	Outlet temperature, °C	Mass flow rate, kg/s	Heat transfer rate, kW
3-Pass	20.27	10.113	222.88
5-Pass	21.19	10.113	261.79
7-Pass	21.96	10.113	294.36

Table 6
High temperature difference case (10 °C inlet / 120 °C shell)

Design	Outlet temperature, °C	Mass flow rate, kg/s	Heat transfer rate, kW
3-Pass	17.66	10.113	323.96
5-Pass	19.00	10.113	380.63
7-Pass	20.20	10.113	431.38

The result demonstrates that the heat transfer performance of the heat exchanger, quantified by the total heat transfer rate (Q), is strongly influenced by both the number of passes and the temperature difference between the shell-side and tube-side fluids. Across all operating conditions,

increasing the number of passes from 3 to 7 consistently enhances energy absorption by the tube-side fluid. This improvement is attributed to two main factors, which are an increased heat transfer surface area and a longer residence time. For example, in the high-temperature difference case, the heat transfer rate rises from 323.96 kW for the 3-pass design to 431.38 kW for the 7-pass design, reflecting a 33 % increase in energy transfer. In addition, the temperature difference between the shell and inlet fluid serves as the primary driving force for heat transfer. Overall, these results highlight the combined effects of geometry and thermal driving force on the heat exchanger's efficiency.

3.4 Effect of Pass Arrangement on Residence Time

The variation in thermal performance among the designs is primarily due to differences in residence time, defined as the average duration a fluid particle remains within the heat transfer domain. With constant inlet flow rate and tube diameter, the residence time increases proportionally with tube length. In the 3-Pass design, the short tube length results in minimal residence time, preventing effective heat transfer to the fluid core. The 5-Pass configuration provides a longer flow path, allowing the thermal boundary layer to develop further, but still insufficient for full core heating. The 7-Pass design maximizes tube length and residence time, enabling the thermal boundary layer to penetrate the bulk fluid and achieve the highest heat absorption. This confirms that increasing the number of passes enhances heat transfer efficiency by extending the fluid's exposure to the heated walls.

3.5 Surface Area and Heat Transfer Efficiency

The geometric configuration of the heat exchanger also influences thermal performance by determining the available heat transfer surface area, A. Since the tube diameter is constant, the total surface area increases with the tube length. The 3-Pass design has the smallest surface area, limiting heat transfer despite the temperature difference between the shell and tube. The 5-Pass configuration increases the total area, allowing more heat absorption, though it remains intermediate. The 7-Pass design maximizes tube surface exposure within the shell, enhancing contact with the hot fluid and achieving the highest heat transfer rate. Thus, increasing the number of passes effectively amplifies the heat transfer surface area, together with extended residence time, which contributes to superior thermal performance.

4. Conclusions

In conclusion, the CFD analysis of conjugate heat transfer in a simplified serpentine heat exchanger demonstrates that both geometric configuration and operating conditions strongly influence thermal performance. Increasing the number of passes from 3 to 7 significantly enhances heat absorption due to longer residence times, allowing the thermal boundary layer to penetrate more effectively into the fluid core. Quantitatively, in the high-temperature difference case (10 °C inlet / 120 °C shell), the total heat transfer rate rose from 323.96 kW to 431.38 kW, reflecting a 33 % improvement. Similar trends were observed in medium and low ΔT cases, confirming the combined effects of extended residence time and increased surface area on heat exchanger efficiency. Overall, the 7-pass design consistently provides the most effective thermal penetration and energy absorption, highlighting the importance of optimizing pass arrangement and flow path length. This

study confirms that CFD is a reliable tool for evaluating conjugate heat transfer and can guide practical design improvements in serpentine heat exchangers.

Acknowledgement
This research was supported by Universiti Tun Hussein Onn Malaysia (UTHM) through Tier 1 (vot Q900)

References

[1] Kim, Jae Seung, Song Hyun Seo, Chang Gyoo Ban, and Kyu Hong Kim. "Conjugate heat transfer analysis of a ram/scramjet with thermal decomposition of the regenerative cooling channel." *International Journal of Heat and Mass Transfer* 244 (2025): 126901. https://doi.org/10.1016/j.ijheatmasstransfer.2025.126901

[2] Ahmed, Zakarya Ali Jilani, Ali BM Ali, Omar Al-Khatib, and Ibrahim Mahariq. "Numerical investigation of passive cooling enhancement using nano-encapsulated phase change materials in electronic thermal management systems." *Thermal Science and Engineering Progress* (2025): 103965. https://doi.org/10.1016/j.tsep.2025.103965

[3] de Araujo Silva, Rafael Alberto, José Ângelo Peixoto da Costa, and Jorge R. Henríquez. "Shell and tube heat exchanger with helical baffles and graphene nanofluids: a numerical thermal–hydraulic analysis." *Chemical Engineering Science* (2025): 122617. https://doi.org/10.1016/j.ces.2025.122617

[4] Jeong, Seung-Min, Kyungjae Lee, Inyoung Yang, Sanghoon Lee, Yang Ji Lee, Jae-Eun Kim, and Jeong-Yeol Choi. "Thermal environment analysis of a scramjet combustor based on pseudo-conjugate heat transfer analysis with combustion." *Journal of Propulsion and Energy* 5, no. 2 (2025): 1-16. https://doi.org/10.6108/JPNE.2025.5.2.001

[5] GaneshKumar, Poongavanam, S. VinothKumar, V. S. Vigneswaran, Seong Cheol Kim, and Vanaraj Ramkumar. "Advancing heat exchangers for energy storage: A comprehensive review of methods and techniques." *Journal of Energy Storage* 99 (2024): 113334. https://doi.org/10.1016/j.est.2024.113334

[6] Chen, Di, and Yosuke Hasegawa. "Level-set based topology optimization in conjugate heat transfer with large solid-to-fluid thermal conductivity ratios." *Applied Thermal Engineering* (2025): 127626. https://doi.org/10.1016/j.applthermaleng.2025.127626

[7] Karaca, Cem, Pablo Olmeda, Xandra Margot, Lucio Postrioti, and Giorgio Baldinelli. *An Investigation of Battery Module Thermal Behavior Based on CFD Simulations and Experimental Tests*. No. 2025-24-0144. SAE Technical Paper, 2025. https://doi.org/10.4271/2025-24-0144

[8] Sheng, Dong-Yuan. "Thermal analysis of continuous casting tundish using a conjugate heat transfer model." *JOM* (2025): 1-8. https://doi.org/10.1007/s11837-025-07196-3

[9] Divakaran, Arun Mambazhasseri, Evangelos Gkanas, James Jewkes, Simon Shepherd, Wissam Jamal, Soroush Faramehr, and Essam Abo-Serie. "3D CFD modelling and experimental validation of conjugate heat transfer in wheel hub motors in micro-mobility vehicles." *Applied Thermal Engineering* 258 (2025): 124430. https://doi.org/10.1016/j.applthermaleng.2024.124430

[10] Ngwa, Mboulé, Longlong Gao, and Baoren Li. "Numerical and experimental investigation of the conjugate heat transfer for a high-pressure pneumatic control valve assembly." *Entropy* 24, no. 4 (2022): 451. https://doi.org/10.3390/e24040451

[11] Tsai, Hung-Tsung, Bo-Jun Lu, Yuh-Ming Ferng, and Yu Sun. "Using CFD modeling to investigate the non-uniform circumferential distribution of heat transfer characteristics in a single-phase helical coiled tube." *Journal of Nuclear Engineering* 6, no. 4 (2025): 41. https://doi.org/10.3390/jne6040041

[12] Zhu, Yongzheng, Shiji Zhao, Yuanye Zhou, Hong Liang, and Xin Bian. "An unstructured adaptive mesh refinement for steady flows based on physics-informed neural networks." *Journal of Computational Physics* (2025): 114283. https://doi.org/10.1016/j.jcp.2025.114283

[13] Perera, Roberto, and Vinamra Agrawal. "Multiscale graph neural networks with adaptive mesh refinement for accelerating mesh-based simulations." *Computer Methods in Applied Mechanics and Engineering* 429 (2024): 117152. https://doi.org/10.1016/j.cma.2024.117152

[14] Li, Yezhan, and Tsubasa Okaze. "Application of polyhedral meshes in large-eddy simulation of building array flow fields within neutral and unstable boundary layers." *Building and Environment* 263 (2024): 111846. https://doi.org/10.1016/j.buildenv.2024.111846

[15] Liu, Huan, Farhad Hussain, Chew Lim Tan, and Manoranjan Dash. "Discretization: An enabling technique." *Data Mining and Knowledge Discovery* 6, no. 4 (2002): 393-423. https://doi.org/10.1023/A:1016304305535

[16] Zulkifli, Zulaika, NH Abdul Halim, Z. H. Solihin, J. Saedon, A. A. Ahmad, A. H. Abdullah, N. Abdul Raof, and M. Abdul Hadi. "The analysis of grid independence study in continuous disperse of MQL delivery system." *Journal of Mechanical Engineering and Sciences* (2023): 9586-9596. https://doi.org/10.15282/jmes.17.3.2023.5.0759

[17] Almohammadi, K. M., D. B. Ingham, L. Ma, and M. Pourkashan. "Computational fluid dynamics (CFD) mesh independency techniques for a straight blade vertical axis wind turbine." *Energy* 58 (2013): 483-493. https://doi.org/10.1016/j.energy.2013.06.012
[18] Abregu, William I. Machaca, Enzo A. Dari, and Federico E. Teruel. "Conjugate heat transfer in spatial laminar-turbulent transitional channel flow." *International Communications in Heat and Mass Transfer* 154 (2024): 107430. https://doi.org/10.1016/j.icheatmasstransfer.2024.107430
[19] Kind, Johannes, Axel Sielaff, and Peter Stephan. "Physical modeling of conjugate heat transfer for multiregion and multiphase systems with the Volume-of-Fluid method." *Engineering with Computers* 41, no. 2 (2025): 761-783. https://doi.org/10.1007/s00366-024-02051-6
[20] Majumder, Sambit, Dipankar Narayan Basu, and Ganesh Natarajan. "Partially-saturated-cells approach for conjugate heat transfer problems." *Computers & Fluids* 274 (2024): 106232. https://doi.org/10.1016/j.compfluid.2024.106232
[21] Ma, Zhendi, Siyu Qin, Yuping Zhang, Wei-Hsin Chen, Guosheng Jia, Chonghua Cheng, and Liwen Jin. "Effects of boundary conditions on performance prediction of deep-buried ground heat exchangers for geothermal energy utilization." *Energies* 16, no. 13 (2023): 4874. https://doi.org/10.3390/en16134874
[22] Reddy, S. D. "CFD analysis on air conditioning effect using K-omega model." *International Journal for Research in Applied Science and Engineering Technology* 13, no. 2 (2025): 366-378. https://doi.org/10.22214/ijraset.2025.66806
[23] Abouzied, Amr S., Ali Basem, Talib K. Ibrahim, Ahmad Almadhor, Khalid Almutairi, Hind Albalawi, Salem Alkhalaf, Dilsora Abduvalieva, Ibrahim Elbadawy, and Samah G. Babiker. "Thermal performance optimization of microchannel heat sinks with triangle wave fin designs and various heat transfer fluids using GA/RSM/TOPSIS." *Case Studies in Thermal Engineering* (2025): 106407. https://doi.org/10.1016/j.csite.2025.106407
[24] Patel, Anand. "Heat exchangers in industrial applications: efficiency and optimization strategies." *International Journal of Engineering Research & Technology (ijert)* 12, no. 09 (2023). https://doi.org/10.37118/ijdr.27172.11.2023
[25] Rahman, Md Atiqur, SM Mozammil Hasnain, and Rustem Zairov. "Assessment of improving heat exchanger thermal performance through implementation of swirling flow technology." *International Journal of Thermofluids* 22 (2024): 100689. https://doi.org/10.1016/j.ijft.2024.100689
[26] Gobinathan, Sashwin Nair, Azizuddin Abd Aziz, Ahmed Nurye Oumer, Mohd Yusof Taib, and Ahmad Basirul Subha Alias. "A review on heat transfer enhancement in a heat exchanger." *Journal of Advanced Research in Fluid Mechanics and Thermal Sciences* 122, no. 2 (2024): 130-145. https://doi.org/10.37934/arfmts.122.2.130145
[27] Amran, Mohd Farid, Sakhr M. Sultan, and C. P. Tso. "A comprehensive review of mixed convective heat transfer in tubes and ducts: Effects of Prandtl number, geometry, and orientation." *Processes* 12, no. 12 (2024): 2749. https://doi.org/10.3390/pr12122749
[28] Liu, Yan, and Liang Li, eds. *Principles of environmental engineering*. Springer Nature Singapore, 2023. https://doi.org/10.1007/978-981-16-9431-8_3
[29] Dogan, Bekir. "Numerical investigation of conjugate heat transfer in circular pipes considering wall thickness, material conductivity, and external convection." *Results in Engineering* 29 (2026): 109236. https://doi.org/10.1016/j.rineng.2026.109236
[30] Ham, Jeonggyun, Eui Kim, Nayoung You, and Honghyun Cho. "Comparison of thermal performance in solution heat exchangers with different chevron angles in absorption system." *Case Studies in Thermal Engineering* 51 (2023): 103598. https://doi.org/10.1016/j.csite.2023.103598
[31] Fares, Mohammad, AL-Mayyahi Mohammad, and AL-Saad Mohammed. "Heat transfer analysis of a shell and tube heat exchanger operated with graphene nanofluids." *Case Studies in Thermal Engineering* 18 (2020): 100584. https://doi.org/10.1016/j.csite.2020.100584